Silver, E. A., Rangin, C., von Breymann, M. T., et al., 1991
Proceedings of the Ocean Drilling Program, Scientific Results, Vol. 124

33. SITE BACKTRACKING AND THE EOCENE-OLIGOCENE CALCITE COMPENSATION DEPTH IN THE CELEBES SEA[1]

Randall B. Smith,[2,3] Marta von Breymann,[4] and Zehui Huang[5]

ABSTRACT

Oceanic crust at Sites 767 and 770 in the northern Celebes Sea is overlain by Eocene and Oligocene pelagic sediments. Brown clay accumulated below the calcite compensation depth (CCD) at the deeper Site 767 throughout this time interval. At the shallower Site 770, nannofossil clay accumulated just above the CCD during middle to late Eocene and early Oligocene time, interrupted by a brief episode of noncalcareous clay deposition in earliest Oligocene time. Depth backtracking of these sites and the alternation of calcareous and noncalcareous sediments at Site 770 indicate that an abrupt lowering of the CCD by as much as 500 m occurred in the Celebes Sea region in earliest Oligocene time. This event was synchronous with an equally abrupt but larger-magnitude drop in the CCD in the Pacific and Atlantic Oceans, which has been attributed to changes in ocean circulation, increasing biological productivity, and the accelerated influx of cold Antarctic Bottom Water into the deep ocean basins. The presence of this paleoceanographic signal in the pelagic sediments at Site 770 indicates that there were open deep-water connections between the Celebes Sea and the Pacific or Indian Oceans during the Eocene and Oligocene. This conclusion supports the notion that the Celebes Sea originated in an open-ocean setting and became a trapped marginal basin as a result of Neogene tectonic events.

INTRODUCTION

Drilling at Ocean Drilling Program Sites 767 and 770 in the northern Celebes Sea confirmed that oceanic crust of late middle Eocene age underlies each site (Shipboard Scientific Party, 1990b and 1990c). Although the sites now lie within a marginal basin largely surrounded by Neogene arc terranes (Rangin and Silver, 1990), the history of sedimentation in the basin is complex. Pelagic, terrigenous turbidite, and volcanogenic sedimentation have each dominated during different stages in the basin's history. Eocene and Oligocene strata at both sites are dominantly pelagic, with little turbidite or volcanogenic sediment. The pelagic character of the first 20 m.y. of the sedimentary record at these sites is persuasive evidence that the crust of the Celebes Sea originated in an open-ocean environment rather than in its present back-arc basin setting (Shipboard Scientific Party, 1990d). We have examined the record of Eocene to early Oligocene pelagic carbonate sedimentation at Sites 767 and 770 for further clues to the early paleoceanographic setting of the Celebes Sea. We conclude that variations in carbonate content at Site 770 record the global drop in the calcite compensation depth (CCD) near the Eocene-Oligocene boundary, suggesting that deep-water connections existed between the Celebes Sea sites and the Pacific or Indian Oceans.

CARBONATE CONTENT OF EOCENE-OLIGOCENE PELAGIC SEDIMENTS

Site 767 was drilled on the deep basin floor (present water depth 4905 m). Brown pelagic claystone with less than 1% carbonate makes up the entire Eocene-Oligocene interval at this site, indicating that deposition occurred well below the CCD. Site 770 was drilled on a raised basement fault block about 400 m shallower (present water depth 4516 m) than Site 767. The relief on the basement surface between the two sites is even greater, about 750 m, reflecting a more condensed sedimentary sequence at Site 770. The middle Eocene through lower Oligocene section at Site 770 consists predominantly of brown nannofossil claystone, but several meters of noncalcareous claystone separates the dated upper Eocene and lower Oligocene calcareous intervals (Fig. 1).

To define the variations in carbonate content through this interval more precisely, we determined the carbonate content of 29 samples from Cores 124-770B-11R through -16R. The data were merged with the shipboard carbonate analyses to produce a database of 44 analyses within the depth range from 360 to 421 meters below seafloor (mbsf), averaging 1 to 2 samples per meter of recovered core. Both shipboard and shore-based analyses were carried out using procedures outlined by the Shipboard Scientific Party (1990a). In routine shipboard work, such analyses have been highly reproducible, with standard deviations for replicate analyses usually less than 1%. The resulting values are listed in Table 1 and plotted on Figure 1.

The carbonate content of the middle to upper Eocene nannofossil claystone in Cores 124-770B-15R and -16R ranges from 5% to 25%, with a mean of 19.2%. The lower Oligocene nannofossil claystone has somewhat higher carbonate contents, ranging from 15% to 45% with a mean of 31.2%. Deposition in both of these intervals took place above, but close to, the CCD, as evidenced by the relatively low carbonate content, moderate to poor preservation of calcareous nannoplankton, and the presence of only dissolution-resistant planktonic foraminifers (Shipboard Scientific Party, 1990c; Nederbragt, this volume).

About 1.7 m of noncalcareous (<1% $CaCO_3$) brown claystone underlies the oldest dated Oligocene calcareous claystone at Site 770 (assigned to nannofossil zone NP21), but the base of this noncalcareous interval was not recovered; a 4.5-m coring gap separates it from the top of the upper Eocene

[1] Silver, E. A., Rangin, C., von Breymann, M. T., et al., 1991. *Proc. ODP, Sci. Results*, 124: College Station, TX (Ocean Drilling Program).
[2] Department of Geology, California State University, Fresno, CA 93740.
[3] Present affiliation: Department of Geology, Sonoma State University, Rohnert Park, CA 94928.
[4] Ocean Drilling Program, 1000 Discovery Drive, College Station, TX 77845-9547, U.S.A.
[5] Department of Geology, Dalhousie University, Halifax, Nova Scotia B3H 3J5, Canada.

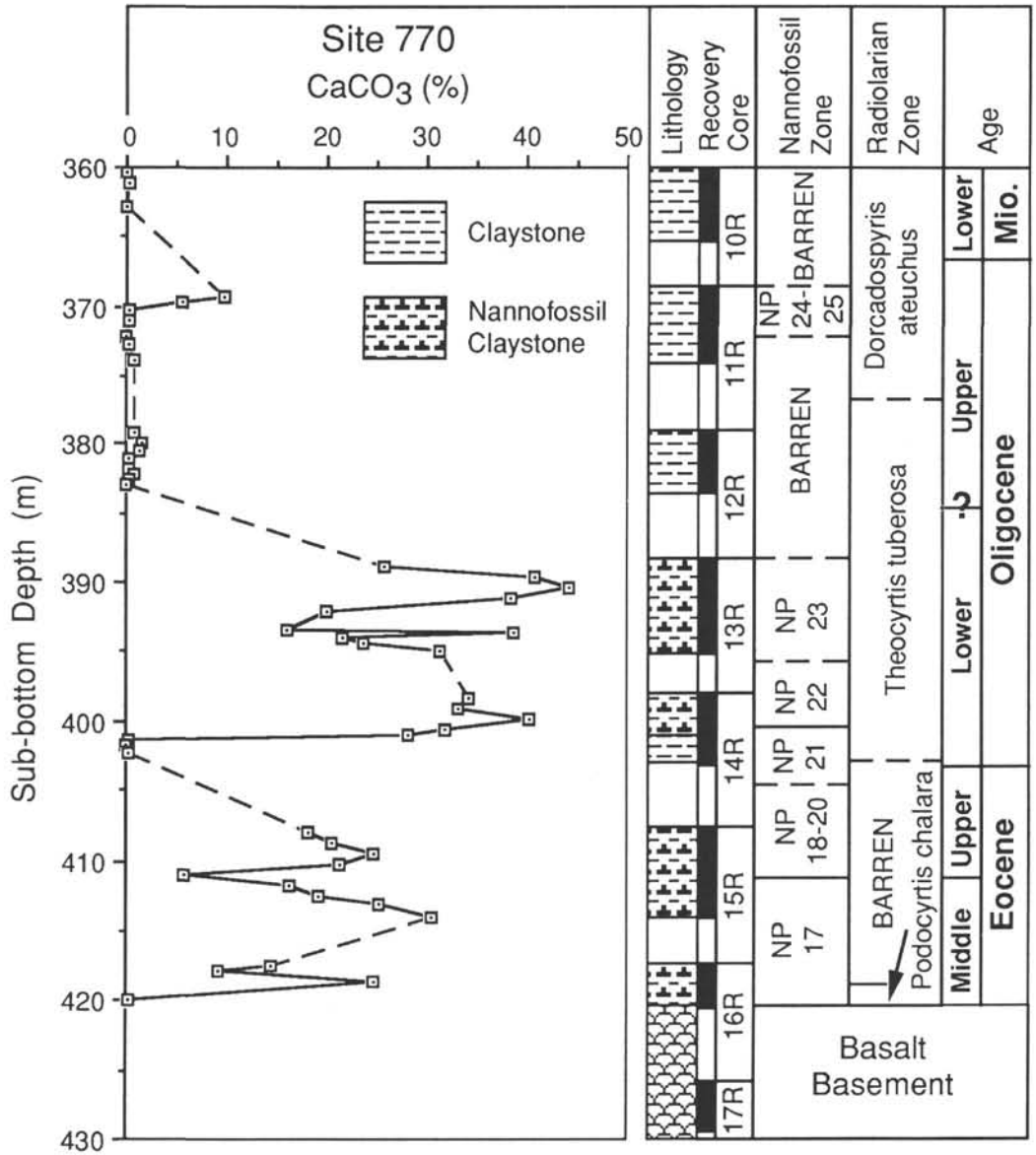

Figure 1. Lithology, paleontologic zonation, and calcium carbonate content of Eocene and Oligocene strata at Site 770. Solid horizontal lines in the zone columns indicate zonal boundaries located within single cores. Dashed horizontal lines in the zone columns indicate zonal boundaries falling between cores, and the boundaries of barren intervals. Lithologic and paleontologic data from Leg 124 Shipboard Scientific Party (1990c).

nannofossil claystone (Fig. 1). Deposition of this claystone occurred during a brief interval near the Eocene-Oligocene boundary when the seafloor lay below the CCD. The lower Oligocene nannofossil claystone is overlain in turn by noncalcareous (<2% $CaCO_3$) brown claystone. From the mid-Oligocene to the present, Site 770 has remained below the CCD.

SEDIMENTATION RATES

We calculated sedimentation rates for the Eocene-Oligocene interval at Site 770 using the depths of biostratigraphic zone boundaries shown in Figure 1 and listed in Table 2. The calcareous nannoplankton zonation was taken from Shipboard Scientific Party (1990c), but the radiolarian zone boundaries have been revised using more recent data (R. Scherer, this volume). For zone boundaries falling within a recovered core interval, the depth of the boundary was taken directly from the shipboard core-description forms. For zone boundaries falling between cores or bounding barren intervals, minimum and maximum depths for the boundaries were assigned. The ages of the boundaries were taken from the Cenozoic time scale of Berggren et al. (1985).

In calculating the sedimentation rates, we assumed that rates were constant within intervals of uniform lithology, and that changes in rate occurred abruptly at lithologic contacts (Fig. 2). Because several of the boundaries between nannofossil claystone and noncalcareous claystone were not recovered, two of the three inflection points fall within zones of no recovery. Rates for the calcareous intervals have the best constraints. The calculated rate for the middle to upper Eocene nannofossil claystone is 4.5 m/m.y., whereas the lower Oligocene nannofossil claystone yields a rate of 8.0 m/m.y., though control exists only in the lower part of the

interval. The noncalcareous intervals show lower rates: about 1.4 m/m.y. for the lower Oligocene claystone, and a poorly-constrained 4.0 m/m.y. for the upper Oligocene claystone. The higher rates of sedimentation for the calcareous intervals reflect enhanced preservation of biogenic carbonate when the seafloor lay above the CCD.

The calculated sedimentation rates can be used to estimate ages for undated portions of the section. By this method the noncalcareous claystone in the lower part of Core 124-770B-14R is interpreted as primarily early Oligocene in age, with the Eocene-Oligocene boundary falling close to the base of the recovered interval. Depths and ages for the boundaries of the nannofossil claystone intervals have been assigned by the same method.

DEPTH BACKTRACKING OF SITES 767 AND 770

Variations in carbonate content of the Eocene and Oligocene sediments at Site 770 are most simply interpreted as the result of thermal subsidence of the oceanic crust and fluctuations in the depth of the CCD through time. We assume that Sites 767 and 770 have followed the typical subsidence curve for oceanic crust (Parsons and Sclater, 1977), and have calculated the paleodepth of individual sedimentary horizons using the method described by Sclater et al. (1985), which takes into account both thermal subsidence and isostatic loading of the crust by sediment deposits. The horizons we have utilized for these calculations are the biozone boundaries listed in Table 2. For boundaries with uncertain depth, we have interpolated a depth based on the calculated sedimentation rates in Fig. 2. The calculated water depths are listed in Table 3 along with parameters used in the calculations, and are plotted in Fig. 3. Sclater et al. (1985) suggest that paleodepths calculated by this method have an accuracy of plus or minus 100 m.

The unsedimented water depth (present basement depth minus the effect of sediment loading) at each site lies below the predicted depth for 42 m.y. oceanic crust. Site 770, on a shallow fault block, is only 64 m deeper than the predicted depth, but Site 770, which is more representative of the basin floor of the Celebes Sea, is 661 m deeper than typical crust of this age. In the method of Sclater et al. (1985) the anomalies (depth offset) are incorporated into the calculation of each paleodepth, under the assumption that they result from an initial depth anomaly rather than an aberrant subsidence history. Crust of early Cenozoic age in the West Philippine Basin shows a similar large depth anomaly, which was attributed by Sclater et al. (1976) to an anomalously thin oceanic crust compared to major ocean basins. However, as pointed out by Weissel (1980), limited seismic refraction data from the Celebes Sea indicate crustal thicknesses resembling those of normal oceanic crust. The cause of the anomalously great depth of the Celebes Sea remains uncertain.

EOCENE-OLIGOCENE FLUCTUATIONS IN THE CCD AT THE CELEBES SEA SITES

On the plots of water depth vs. age for Sites 767 and 770 (Fig. 3) we have indicated times of calcareous and noncalcareous sedimentation at the two sites as a means of tracking the changing depth of the CCD through the Eocene and Oligocene. The time limits for these depositional events at Site 770 have been approximated from the sedimentation rate calculations discussed above, and may be in error by as much as 1 m.y. Between 42 and 39 Ma, the two sites straddled the CCD, which was thus limited to between 2600 and 3100 m. At about 38.7 Ma Site 770 intersected the CCD at a water depth of 3200 m, suggesting that the middle Eocene CCD was between 3000 and 3100 m. Site 770 remained below the CCD until about 35 Ma at which time calcareous deposition resumed at Site 770 at a water depth of 3500 m. At 33 Ma, Site 770 subsided below the CCD for the last time at a water depth of 3600 m.

The data from Sites 767 and 770 document a descent of the CCD by about 500 m between the middle Eocene and early Oligocene, with most of this drop occurring rapidly in earliest Oligocene time. A significant deepening of the CCD occurred near the Eocene/Oligocene boundary in all major oceans, though the magnitude of the drop apparently varied from ocean to ocean (Fig. 4). The deepening was most pronounced and abrupt in the Pacific, with the equatorial Pacific CCD falling by 1600 m and the non-equatorial CCD dropping about 1000 m (van Andel et al., 1975). CCD fluctuations for this time interval are less well-constrained for the Indian Ocean, but the descent of the CCD from Eocene to Oligocene time appears to be more gradual (van Andel, 1975). The inferred middle Eocene depth of the Celebes CCD (3000 to 3100 m) is very close to that of the Pacific Ocean for the same time frame (3200 to 3400 m), and considerably shallower than that of Indian and Atlantic Oceans (van Andel, 1975; van Andel et al., 1975). However, the Oligocene depth of the Celebes CCD was between 3600 and 3800 m, substantially shallower than that of the equatorial or non-equatorial Pacific.

EOCENE-OLIGOCENE SEDIMENT ACCUMULATION RATES AT SITE 770

As a further means of comparing the history of pelagic sedimentation in the Celebes Sea with that of the surrounding oceans, we have utilized bulk density and porosity data to determine sediment accumulation rates in terms of mass per unit area for the Eocene-Oligocene section at Site 770, using the procedure outlined by van Andel et al. (1975), Worsley and Davies (1979), and Thunell and Corliss (1986).

We first calculated average total accumulation rates for the four intervals of inferred constant sedimentation rate (Fig. 2) between 42 and 30 Ma, using average values of bulk density and porosity determined from routine shipboard determinations of these parameters (Shipboard Scientific Party, 1990c). The parameters and mathematical relationship used and the resulting average accumulation rates are given in Table 4.

The accumulation rates for the nannofossil claystone intervals were 0.68 $g/cm^2 \cdot 10^3$ yr for the middle to upper Eocene section and 1.08 $g/cm^2 \cdot 10^3$ yr for the lower Oligocene section. The claystone intervals that accumulated below the CCD show lower accumulation rates, ranging from 0.20 $g/cm^2 \cdot 10^3$ yr for the lower Oligocene to 0.48 $g/cm^2 \cdot 10^3$ yr for the upper Oligocene. The low sediment accumulation rates for the Eocene through early Oligocene interval at Site 770 are comparable to rates in the equatorial Pacific for the same time interval (< 1.00 $g/cm^2 \cdot 10^3$ yr; Worsley and Davies, 1979). The Pacific data indicate that rates of accumulation above 1.0 $g/cm^2 \cdot 10^3$ yr were attained only in portions of the eastern and western tropical Pacific with high rates of carbonate sedimentation.

We also utilized the carbonate content data (Table 1) to analyze variations in carbonate accumulation rates at Site 770. For each analyzed sample, the carbonate accumulation rate (R_c) was calculated using the relationship given in Table 1. Because bulk density and porosity values were not available for all samples, we used an indirect means to derive these values. Plots of shipboard determinations of bulk density (Fig. 5A) and porosity (Fig. 5B) show approximately linear relationships between these parameters and sub-bottom depth for the interval of interest. After excluding data points that we interpreted to be anomalous, we used simple linear regression

Table 1. Carbonate content, sedimentation rate, and calculated carbonate accumulation rates for Eocene and Oligocene strata, Site 770. Carbonate accumulation rates were calculated using the method of Worsley and Davies (1979) and Thunell and Corliss (1986). Values of bulk density and porosity used in the calculations were extrapolated from the approximately linear downhole variation in these parameters.

Sample Number Leg-Site/Hole: Core-Section, interval (cm)	Depth (mbsf)	$CaCO_3$ (%)	Data source[a]	(D) Calculated Bulk density (g/cm^3)	(P) Calculated porosity (%)	(R) Sedimentation rate ($cm/10^3$ yr)	(R_C) Carbonate accumulation rate[b] ($g/cm^2 \cdot 10^3$ yr)
124-770B-:							
10R-01, 111--113	360.41	0.1	S	1.73	65.3	0.40	0.000
10R-02, 26--28	361.06	0.2	S	1.73	65.1	0.40	0.001
10R-03, 51--53	362.81	0.1	S	1.74	64.5	0.40	0.000
11R-01, 32--34	369.22	9.6	P	1.77	62.2	0.40	0.044
11R-01, 80--82	369.70	5.4	S	1.77	62.1	0.40	0.025
11R-01, 128--130	370.18	0.4	P	1.78	61.9	0.40	0.002
11R-02, 53--55	370.93	0.3	S	1.78	61.6	0.40	0.001
11R-03, 21--23	372.11	0.0	P	1.79	61.2	0.40	0.000
11R-03, 89--91	372.79	0.2	S	1.79	61.0	0.40	0.001
11R-04, 50--52	373.90	0.9	P	1.80	60.6	0.40	0.004
12R-01, 52--54	379.12	0.7	S	1.82	58.8	0.40	0.003
12R-01, 128--130	379.88	1.5	P	1.83	58.5	0.40	0.007
12R-02, 40--42	380.50	1.2	P	1.83	58.3	0.40	0.006
12R-02, 103--105	381.13	0.3	S	1.83	58.1	0.40	0.001
12R-03, 19--21	381.79	0.4	P	1.84	57.8	0.40	0.002
12R-03, 60--62	382.20	0.7	P	1.84	57.7	0.40	0.003
12R-03, 104--106	382.64	0.2	P	1.84	57.6	0.40	0.001
12R-03, 142--144	383.02	0.1	P	1.84	57.4	0.40	0.000
13R-01, 63--65	388.83	25.7	S	1.87	55.4	0.80	0.268
13R-01, 134--136	389.54	40.8	P	1.88	55.1	0.80	0.427
13R-02, 58--60	390.28	44.2	P	1.88	54.9	0.80	0.466
13R-02, 138--140	391.08	38.3	S	1.88	54.6	0.80	0.405
13R-03, 88--90	392.08	20.0	S	1.89	54.3	0.80	0.213

Table 1 (continued).

13R-04, 73--75	393.43	16.1	P	1.89	53.8	0.80	0.173
13R-04, 88--90	393.58	38.6	S	1.90	53.7	0.80	0.415
13R-04, 119--121	393.89	21.6	P	1.90	53.6	0.80	0.232
13R-05, 22--24	394.42	23.8	P	1.90	53.4	0.80	0.258
13R-05, 69--71	394.89	31.4	P	1.90	53.3	0.80	0.340
14R-01, 50--52	398.40	34.3	P	1.92	52.1	0.80	0.380
14R-01, 124--126	399.14	33.2	S	1.92	51.8	0.80	0.370
14R-02, 50--52	399.90	40.2	P	1.93	51.5	0.80	0.450
14R-02, 122--124	400.62	31.8	S	1.93	51.3	0.80	0.358
14R-03, 15--17	401.05	28.1	P	1.93	51.1	0.80	0.317
14R-03, 46--48	401.36	0.2	P	1.94	51.0	0.14	0.000
14R-03, 91--93	401.81	0.0	P	1.94	50.9	0.14	0.000
14R-03, 141--143	402.31	0.3	S	1.94	50.7	0.14	0.001
15R-01, 39--41	407.99	18.2	S	1.97	48.7	0.45	0.120
15R-01, 120--122	408.80	20.5	P	1.97	48.4	0.45	0.136
15R-02, 49--51	409.59	24.7	P	1.98	48.2	0.45	0.165
15R-02, 121--123	410.31	21.3	S	1.98	47.9	0.45	0.143
15R-03, 48--50	411.08	5.7	P	1.98	47.6	0.45	0.038
15R-03, 119--121	411.79	16.3	P	1.99	47.4	0.45	0.110
15R-04, 45--47	412.55	19.3	P	1.99	47.1	0.45	0.131
15R-04, 111--113	413.21	25.3	S	2.00	46.9	0.45	0.172
15R-05, 40--42	414.00	30.6	P	2.00	46.6	0.45	0.210
16R-01, 26--28	417.56	14.4	S	2.02	45.4	0.45	0.101
16R-01, 65--67	417.95	9.2	P	2.02	45.2	0.45	0.065
16R-01, 123--125	418.53	24.6	P	2.02	45.0	0.45	0.173
16R-03, 32--34	420.02	0.2	S	2.03	44.5	0.45	0.001

[a] S = Shipboard analysis, P = Post-cruise analysis (this study)

[b] $Rc = (\%CaCO_3 \bullet 0.01) \bullet (D - 0.01025 \bullet P) \bullet S$

Table 2. Sub-bottom depths and ages of biozone boundaries used in sedimentation rate calculations, Sites 770 and 767. Biostratigraphic data are from Shipboard Scientific Party (1990b, 1990c). Age assignments for zone boundaries are from Berggren et al. (1985).

	Zone Boundary	Minimum Depth (mbsf)	Maximum Depth (mbsf)	Age (Ma)
Site 770				
1	Top Dorcadospyris ateuchus Zone	?	359	23
2	Top NP 23	370	388	30
3	Top Theocyrtis tuberosa Zone	374	379	31
4	Top NP 22	395	398	34.6
5	Top NP 21	400	400	35
6	Base NP 21	401	408	37
7	Top NP 17	412	412	40
8	Podocyrtis chalara Zone	421	421	42
Site 767				
3	Top Theocyrtis tuberosa Zone	738	744	31
8	Podocyrtis chalara Zone	785	785	42

analysis to find a best-fit line through the data points for each parameter. Bulk density and porosity values from these best-fit lines were then assigned for the depths corresponding to each carbonate sample. These values are listed in Table 1 along with the calculated carbonate accumulation rates, which are also plotted in Figure 6.

Carbonate accumulation rates for the middle to upper Eocene nannofossil claystone at Site 770 range from 0.04 to 0.21 $g/cm^2 \cdot 10^3$ yr, with a mean of 0.13 $g/cm^2 \cdot 10^3$ yr. Rates are significantly higher for the lower Oligocene calcareous interval, ranging from 0.17 to 0.46 $g/cm^2 \cdot 10^3$ yr, with an average of 0.34 $g/cm^2 \cdot 10^3$ yr. Although the calculated values are sensitive to the choice of interval sedimentation rate, which is less well constrained for the lower Oligocene interval, the combination of higher carbonate content and higher sedimentation rate for the lower Oligocene section suggests that the higher carbonate accumulation rates for this interval are real. By comparison, early Oligocene carbonate accumulation rates in the equatorial zone of high productivity in the central Pacific ranged from 0.25 to over 0.50 $g/cm^2 \cdot 10^3$ yr (Worsley and Davies, 1979); rates for Site 770 are near the low end of this range.

The calculation of carbonate accumulation rates from carbonate content data removes the effect of variations in supply of the non-carbonate sediment components. The variation in carbonate accumulation rates can then be interpreted in terms of changes in rate of supply or dissolution of pelagic carbonate. With our limited data we are unable to determine the relative contribution of either factor to the observed variation in accumulation rates at Site 770. Thunell and Corliss (1986) found significant increases in carbonate accumulation rates near the Eocene-Oligocene boundary at western Pacific and eastern Indian Ocean Deep Sea Drilling Project sites that were well above the compensation depth. They concluded that increase in surface water productivity coincided with the global deepening of the CCD at the Eocene-Oligocene boundary, and that both were linked to more vigorous surface-water and deep-water circulation resulting from cooling climate.

CONCLUSIONS

During the Eocene and early Oligocene, sediments of typical open-ocean pelagic character were deposited at Sites 767 and 770 in the northern Celebes Sea. We observe that these sediments record a major global paleoceanographic signal in the form of a dramatic deepening of the level of the calcite compensation depth near the Eocene-Oligocene boundary. This global deepening has been attributed to more vigorous oceanic circulation, higher biological productivity, and the influx of cold Antarctic Bottom Water into the deep ocean basins (van Andel, 1975; Corliss and Keigwin, 1986; Thunell and Corliss, 1986). The synchronous deepening of the CCD at the Celebes Sea sites and in the major ocean basins indicates that the changes in climatic and oceanographic factors causing the deepening affected the Celebes Sea region as well as the Pacific and Indian Ocean. We interpret this as evidence that there was open communication and mixing of surface and deep-water masses between the Celebes Sea region and the Pacific or Indian Oceans during the Eocene and Oligocene. In contrast, the Celebes Sea is presently enclosed by volcanic arc and accretionary terranes and has no deep-water connections with either ocean. This change in paleoceanographic setting lends support to the idea that the Celebes Sea was originally part of one of the major ocean basins, and

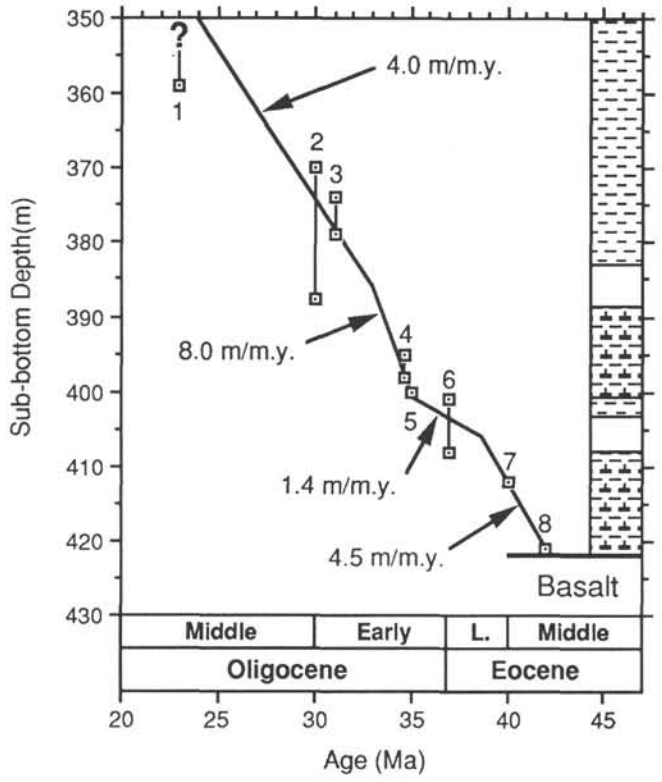

Figure 2. Sedimentation rates for the Eocene and Oligocene section at Site 770 calculated from biostratigraphic data. Numbered zonal boundaries are listed in Table 2. Lithologic symbols are the same as in Figure 1. Rates were plotted assuming constant rate within intervals of uniform lithology and changes in rate coinciding with contacts between calcareous and noncalcareous intervals. Depth intervals and corresponding time intervals for which the calculated rates apply are listed in Table 3.

attained its present marginal basin setting as a result of Neogene tectonic reorganization of the region. The abrupt nature of the CCD drop at the Celebes Sea sites (Fig. 4) suggests a closer affinity with the Pacific Ocean than with the Indian Ocean.

ACKNOWLEDGMENTS

R. B. Smith thanks the Geology Department at Tulane University for facilitating his participation on Leg 124. The manuscript was significantly improved by reviews from Kurt Grimm (University of California, Santa Cruz) and Tj. H. van Andel (Stanford University).

REFERENCES

Berggren, W. A., Kent, D. V., Flynn, J. J., and Van Couvering, J. A., 1985. Cenozoic geochronology. *Geol. Soc. Am. Bull.*, 96:1407–1418.

Corliss, B. H., and Keigwin, L. D., 1986. Eocene/Oligocene paleoceanography. *In* Hsü, K. J. (Ed.), *Mesozoic and Cenozoic Oceans:* Am. Geophys. Union Geodyn. Ser., 15:101–118.

Parsons, B., and Sclater, J. G., 1977. An analysis of the variation of ocean floor bathymetry and heat flow with age. *J. Geophys. Res.*, 82:803–827.

Rangin, C., and Silver, E., 1990. Geological setting of the Celebes and Sulu Seas. *In* Rangin, C., Silver, E. A., et al., *Proc. ODP, Init. Repts.*, 124: College Station, TX (Ocean Drilling Program), 35–42.

Sclater, J. G., Karig, D. E., Lawver, L. A., and Louden, K., 1976. Heat flow, depth, and crustal thickness of the marginal basins of the south Philippine Sea. *J. Geophys. Res.*, 81:309–318.

Sclater, J. G., Meinke, L., Bennett, A., and Murphy, C., 1985. The depth of the ocean through the Neogene. *In* Kennett, J. P. (Ed.), *The Miocene Ocean: Paleoceanography and Biogeography:* Mem. Geol. Soc. Am., 163:1–20.

Shipboard Scientific Party, 1990a. Explanatory notes. *In* Rangin, C., Silver, E. A., et al., *Proc. ODP, Init. Repts.*, 124: College Station, TX (Ocean Drilling Program), 7–33.

_____, 1990b. Site 767. *In* Rangin, C., Silver, E. A., et al., *Proc. ODP, Init. Repts.*, 124: College Station, TX (Ocean Drilling Program), 121–193.

_____, 1990c. Site 770. *In* Rangin, C., Silver, E. A., et al., *Proc. ODP, Init. Repts.*, 124: College Station, TX (Ocean Drilling Program), 343–397.

_____, 1990d. Summary of shipboard results. *In* Rangin, C., Silver, E. A., et al., *Proc. ODP, Init. Repts.*, 124: College Station, TX (Ocean Drilling Program), 415–419.

Thunell, R. C., and Corliss, B. H., 1986. Late Eocene-early Oligocene carbonate sedimentation in the deep sea. *In* Pomerol, C., and Premoli-Silva, I. (Eds.), *Terminal Eocene Events:* New York (Elsevier), Developments in Palaeontology and Stratigraphy, 9:363–380.

van Andel, T. H., 1975. Mesozoic/Cenozoic calcite compensation depth and the global distribution of calcareous sediments. *Earth Planet. Sci. Lett.*, 26:187–194.

van Andel, T. H., Heath, G. R., and Moore, T. C., Jr., 1975. Cenozoic history and paleoceanography of the central equatorial Pacific. *Mem. Geol. Soc. Am.*, 143:1–134.

Weissel, J. K., 1980. Evidence for Eocene oceanic crust in the Celebes Basin. *In* Hayes, D. E. (Ed.), *The Tectonic and Geologic Evolution of Southeast Asian Seas and Islands*. Am. Geophys. Union, Geophys. Monogr. Ser., 23:37–47.

Worsley, T. R., and Davies, T. A., 1979. Cenozoic sedimentation in the Pacific Ocean: steps toward a quantitative evaluation. *J. Sediment. Petrol.*, 49:1131–1146.

Date of initial receipt: 31 May 1990
Date of acceptance: 19 December 1990
Ms 124B-140

Table 3. Water depths for selected times during the Eocene and Oligocene at Sites 767 and 770. Depths were calculated using the method of Sclater et al. (1985). Parameters used in the calculations for each site are shown at right, and density values used for both sites are shown at the bottom.

Age (Ma)	Sub-bottom Depth (mbsf)	Sedimented Water Depth (m)
Site 770:		
42	421	2564
40	412	3053
37	403	3335
35	400	3477
31	378	3698
30	373	3747
Site 767:		
42	785	3160
31	741	4294

Site Parameters	
Site 770:	
Present water depth:	4516 m
Basement depth:	421 m
Basement age:	42 Ma
Average sediment density[a]:	1.6 g/cm^3
Calculated unsedimented water depth:	4833 m
Offset from predicted depth:	+64 m
Site 767:	
Present water depth:	4906 m
Basement depth:	786 m
Basement age:	42 Ma
Average sediment density[a]:	1.8 g/cm^3
Calculated unsedimented water depth:	5429 m
Offset from predicted depth:	+661 m

[a] Other densities used in calculations (g/cm^3): Mantle = 3.33 Seawater = 1.03 Eocene-Oligocene Sediment = 1.9

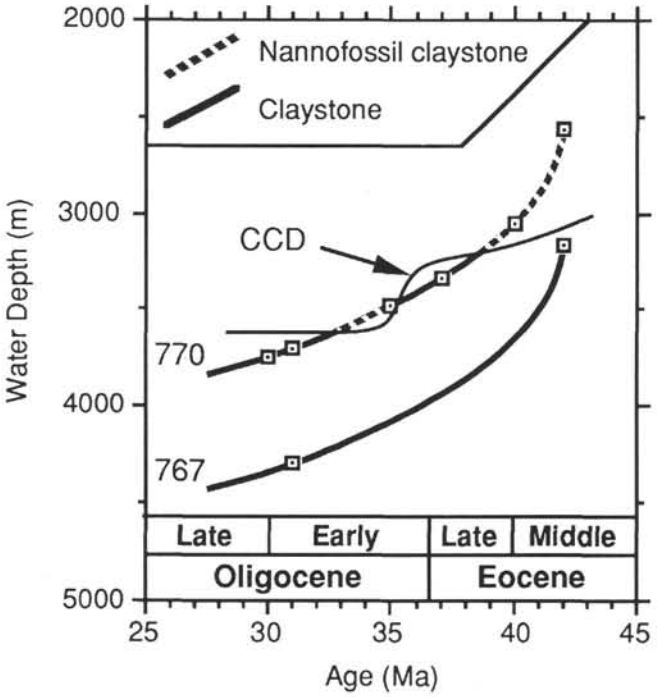

Figure 3. Calculated change in water depth through Eocene and Oligocene time for Celebes Sea Sites 767 and 770. Sedimented water depths were calculated using the method of Sclater et al. (1985); data are tabulated in Table 4.

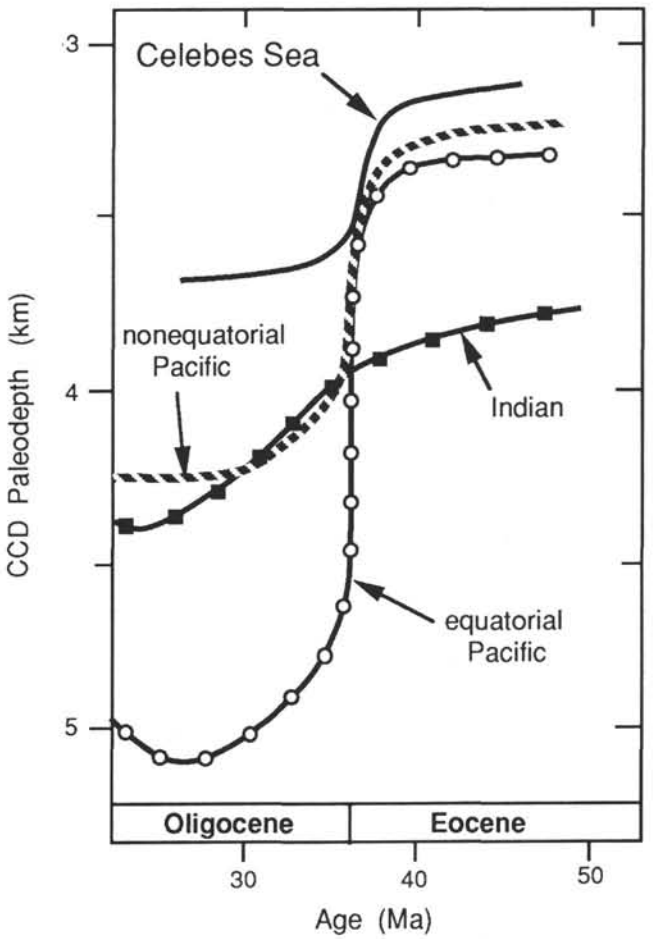

Figure 4. Variation of the calcite compensation depth (CCD) with time for the Celebes Sea sites (767 and 770, this study), the equatorial and nonequatorial Pacific Ocean (van Andel et al., 1975), and the Indian Ocean (van Andel, 1975).

Table 4. Sedimentation rates and average mass accumulation rates for intervals of the Eocene through Oligocene section at Site 770. Accumulation rates were calculated using the method of van Andel et al. (1975) and Worsley and Davies (1979).

Sub-bottom Depth Interval (mbsf)	Time Interval (Ma)	(D) Average Bulk Density (g/cm^2)	(P) Average Porosity (%)	(S) Sedimentation Rate (cm/1000 yr)	(R) Accumulation Rate[a] ($g/cm^2 \cdot 1000$ yr)
368 to 386	30 to 33	1.81	59.5	0.40	0.48
386 to 401	33 to 35.1	1.90	53.8	0.80	1.08
401 to 406	35.1 to 38.7	1.95	50.3	0.14	0.20
406 to 421	38.7 to 42	2.00	46.8	0.45	0.68

[a] $R = (D - 0.01025 \cdot P) \cdot S$

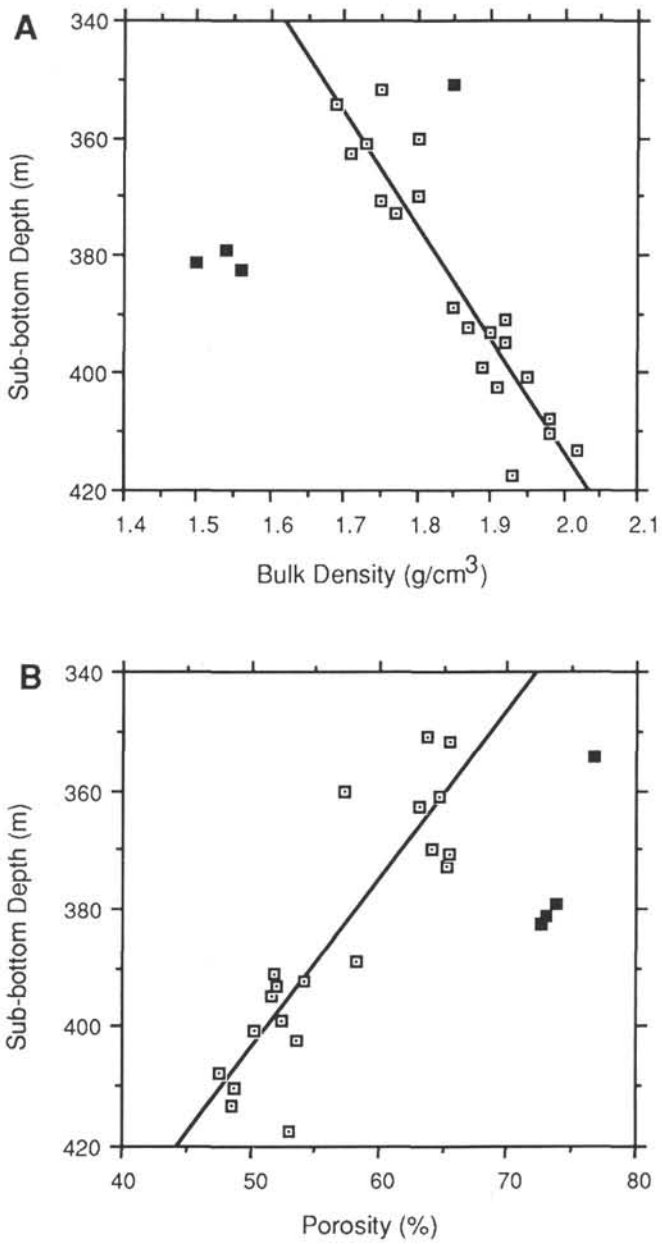

Figure 5. Plots of sediment bulk density (**A**) and sediment porosity (**B**) vs. sub-bottom depth for the lower part of Hole 770B. Data from Leg 124 Shipboard Scientific Party (1990c). Open symbols are values considered reliable, which were used to fit linear regressions lines to the data. Solid symbols are values judged to be unreliable; they were excluded from the regression analysis. The plotted regression lines and equations describe the average change in bulk density and porosity with depth in the hole.

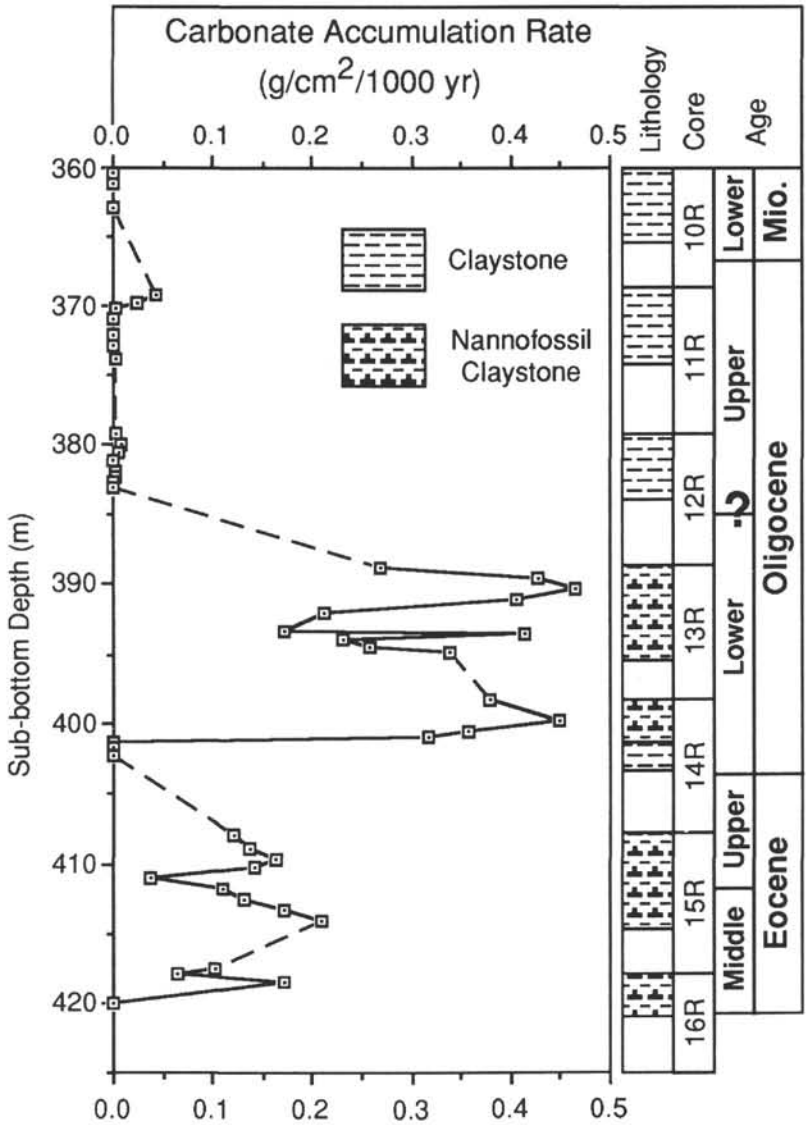

Figure 6. Calculated carbonate accumulation rates for the Eocene and Oligocene section at Site 770.